ISTITUTO DI ANALISI DEI SISTEMI ED INFORMATICA
CONSIGLIO NAZIONALE DELLE RICERCHE

A. Bertuzzi, A. Gandolfi

CELL KINETICS IN A TUMOUR CORD

R. 473 Ottobre 1998

Alessandro Bertuzzi – Istituto di Analisi dei Sistemi ed Informatica del CNR, viale Manzoni 30 - 00185 Roma, Italy. Email : bertuzzi@iasi.rm.cnr.it.

Alberto Gandolfi – Istituto di Analisi dei Sistemi ed Informatica del CNR, viale Manzoni 30 - 00185 Roma, Italy. Email : gandolfi@iasi.rm.cnr.it.

This work partially supported by the Progetto Strategico CNR "Metodi e Modelli Matematici nello Studio dei Fenomeni Biologici".

Istituto di Analisi dei Sistemi ed Informatica, CNR
viale Manzoni 30
00185 ROMA, Italy

tel. ++39-06-77161
fax ++39-06-7716461
email: iasi@iasi.rm.cnr.it
URL: http://www.iasi.rm.cnr.it

Abstract

In some tumours, the viable cells grow around blood vessels forming cylindrical structures called tumour cords, which are surrounded by regions of necrosis. In the present paper we propose a mathematical model for the cell kinetics in a tumour cord at the stationary state. Both proliferating cells and quiescent cells are considered, and the proliferating cell population is structured by age. Cell migration towards cord periphery is accounted for from a continuum viewpoint. The age distribution of proliferating cells, the fraction of cells in S phase, the growth fraction and the velocity along the cord radius are computed. The predictions of the model are compared to literature data obtained from two experimental rat hepatomas. The model was used to compute the profile of the oxygen tension within the cord. Possible modifications and extensions are also presented.

Key words: Cell kinetics, age-structured populations, solid tumours, tumour vascularization, oxygenation.

1. Introduction

In the growth of solid tumours an initial avascular phase is followed by the development, which is stimulated by factors released by the tumour itself (Folkman, 1985), of a vascular network inside the tumour, supplying oxygen and nutrients necessary for the further growth of the tumour mass (Chaplain, 1997). This phase is called the vascular phase of the tumour growth. As the size becomes larger, the tumour vasculature appears to be inadequate (Warren, 1979) to supply all the tumour cells, so that the cells most remote from vessels undergo necrosis. Large regions of necrosis have indeed been evidenced by many histological studies (Thomlinson and Gray, 1955; Folkman, 1974).

In most neoplastic tissues, the complex and irregular structure of the tumour vascular system makes it difficult to study the relationship between vasculature and cell proliferation and, ultimately, between vasculature and tumour growth. However, in some tumours, the tumour architecture shows a certain degree of regularity. Malignant cells proliferate around fairly straight blood vessels, forming cylindrical arrangements of viable tumour cells named *tumour cords* (Tannock, 1968; Hirst and Denekamp, 1979; Hirst *et al.*, 1982; Moore *et al.*, 1984; Moore *et al.*, 1985; Falkvoll, 1990; Hirst *et al.*, 1991). Oxygen tension and the concentration of nutrients, such as glucose, decay radially within the cord and, when they fall below some critical values, cell death occurs, so the cords are surrounded by regions of necrosis. The mean thickness of the cords (*i.e.*, the distance between the vessel wall and the first layer of necrotic cells) in different tumours has been found to be 60–120 μm, whereas the mean radius of the central vessel has been found to be 10–40 μm. The decreasing value along the cord radius of the fraction of cells in S phase, which is given by the labelling index measured a short time after a pulse injection of tritiated thymidine, shows that cell proliferation within the cord slows down moving towards the periphery (Tannock, 1968; Hirst and Denekamp, 1979; Moore *et al.*, 1984). This slowing down of the proliferation could be related to the decrease of the concentration of some critical chemical(s).

The cord is a dynamic structure, because cells continuously proliferate within the cord. Cells are pushed by dividing cells and migrate outwards, and eventually move into the necrotic zone. Evidence of this migration was obtained by measuring the time course of the labelling index of cells in the most external region of the cord (Tannock, 1968; Hirst and Denekamp, 1979; Hirst *et al.*, 1982; Moore *et al.*, 1984). Of course, a fraction of the dividing cells also contributes to the longitudinal growth of the cord, but longitudinal growth appears to be a slower phenomenon (Tannock, 1968), possibly related to the growth of new vessels, and is neglected in the present work.

In the present paper, following a suggestion given in McElwain and Pettet (1993), we propose a mathematical model for the cell kinetics in a tumour cord in the stationary state, when the cord has attained its maximal radius compatible with the supply of vital substances from the central vessel, and the structure of the cell population becomes time-invariant. Both proliferating cells and quiescent cells are considered, and cell migration towards cord periphery is accounted for from a continuum viewpoint in a simple geometry. Model predictions about the structure of the cell population within the cord and the cell migration are compared to data obtained from two experimental rat hepatomas (Moore *et al.*, 1984). The model, by yielding a better knowledge of the structure of the cell population, could be used to improve the computation of the profile of oxygen tension within the cord. An example of this computation is given. Possible modifications and extensions of the model are also presented.

2. Assumptions

Let us consider a tumour cord around a blood vessel of radius r_0. The tumour cord has cylindrical symmetry, and r will denote the radial position within the cord, as shown in Fig. 1. Changes of variables along the axial direction are neglected.

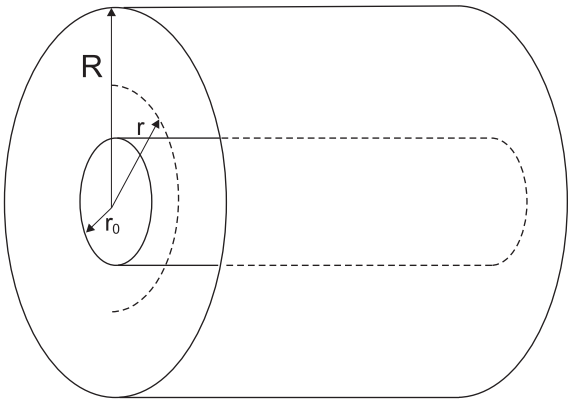

Fig. 1. Schematic representation of a tumour cord.

Experimental data on the expression of proliferation markers (Danova *et al.*, 1990) suggest the presence of quiescent (out-of-cycle) cells in tumours. Thus we consider the population of viable tumour cells in the cord as composed by proliferating (P) cells and quiescent (Q) cells. The population of the cycling cells will be structured by age, and will be described by the cell density with respect to age and volume $n(a,r,t)$, $n(a,r,t)\,da$ being the number of cells with age between a and $a+da$ in the unit volume at position r and time t. Q cells are described by the density $n_Q(r,t)$, which gives the number of quiescent cells in the unit volume at position r and time t. The distinction between P and Q cells and the consideration of the age of P cells are important because the response of tumour cells to treatment usually differs according to their cycling or quiescent status and according to the cell cycle phase.

In this paper we assume a very simplified cell cycle structure (see Fig. 2) in which the different environmental conditions within the cord are assumed to affect only the transition to quiescence. The variability of phase transit times is disregarded, so all proliferating cells traverse the cycle in the same time T_c and the cell age a, counted from cell entry into G1, is such that $0 \le a \le T_c$. The cells that are born at position r and time t may enter the cycle with probability $\theta(r,t)$ or become quiescent with probability $1-\theta(r,t)$; there is no recruitment of quiescent cells into the cycle. The dependence of θ on r and t reflects the dependence of cell decycling on the concentration of oxigen and/or nutrients within the cord. The observed decrease of proliferation along the cord radius will be accounted for by decreasing the value of θ with r. Cell death within the cord is neglected and necrosis may occur only outside the cord.

Cell fluxes within the cord are assumed to be radially directed, and there is no cell flux across the vessel wall. We assume that cell fluxes can be described by a single velocity field $u(r,t)$, common to all the cells, independently of cell age and proliferating or quiescent status. This means that cells are assumed to behave as a single "cellular fluid", and that cell motions of diffusion type are excluded. The assumption of absence of diffusion can however be relaxed, as will be seen in section 6. The product of $u(r,t)$ times the number of cells per unit volume gives

the cell flux per unit area in the direction of r increasing, across a cylindrical surface of radius r. Since the velocity field is specified by a scalar field, the conservation laws will lead to a purely kinematic approach (Gandar *et al.*, 1990).

Histological observations of tumour cords show that the tumour cells are rather closely packed within the cord, thus suggesting that the cell volume density (*i.e.*, the volume occupied by cells per unit volume) could be constant along the cord radius and near to the unity. The assumption of constant cell volume density has been made in various mathematical models of multicellular spheroids and prevascular tumours (see *e.g* Greenspan, 1972; McElwain and Ponzo, 1977; Adam and Maggelakis, 1990). Measurements of the number of cells per unit volume in histological sections of tumour cords pointed out that this density remains rather unchanged from the inner to the outer regions of the cord (Moore *et al.*, 1984; Moore *et al.*, 1985), so that we will assume here constant the total cell density, and will discuss in section 6 the assumption of constant cell volume density. Note that, since the cells have different volumes according to their age or to their being quiescent, the mean volume of the cells may change with r, so that the cell volume density is not necessarily proportional to the total cell density.

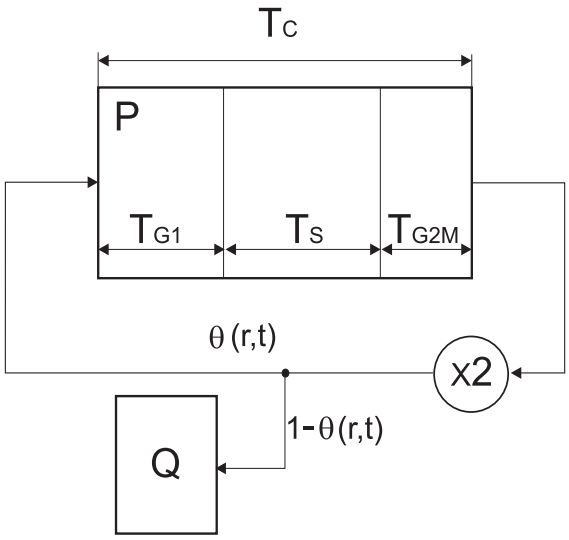

Fig. 2. Block diagram of the cell population model. For the symbols see the text.

3. Stationary structure of the cell population in the cord

The first formulation of a population model with spatial dependence and structured by age can be found in Gurtin 1973. Following Gurtin (1973) and Gurtin and McCamy (1977), and according to the assumed cell cycle structure, the conservation equations for the cell densities in the cord can be written as

$$\frac{\partial n}{\partial t} + \frac{\partial n}{\partial a} + \frac{1}{r}\frac{\partial}{\partial r}(run) = 0 \tag{1}$$

$$n(0, r, t) = 2\theta(r, t)n(T_c, r, t) \tag{2}$$

$$\frac{\partial n_Q}{\partial t} + \frac{1}{r}\frac{\partial}{\partial r}(run_Q) = 2(1 - \theta(r, t))n(T_c, r, t)\,. \tag{3}$$

In this paper, our interest is focussed on the stationary state, *i.e.* the state in which the radius of the cord, R, is constant with time, and all the variables are time-invariant: $n(a,r,t)=n(a,r)$, $a\in[0,T_c]$, $r\in(r_0,R)$, and similarly for n_Q, u, and θ (with $0<\theta(r)\leq 1$). We notice that all the available experimental data are likely to refer to cords in this state.

From the conservation laws, we have that at the stationary state the functions n, n_Q and u must satisfy the following equations:

$$\frac{\partial n}{\partial a}+\frac{1}{r}\frac{\partial}{\partial r}(run)=0 \tag{4}$$

$$n(0,r)=2\theta(r)n(T_c,r) \tag{5}$$

$$\frac{1}{r}\frac{d}{dr}(run_Q)=2(1-\theta(r))n(T_c,r)\,. \tag{6}$$

It is rather easy to see that the scalar velocity field u and the cell densities n and n_Q are not independent functions, and that both u and n_Q can be computed from n. Under the assumption of constant total cell density along the radius, the following expression for u can be obtained. By integrating Eq. (4) with respect to age and taking into account (5) and (6), we have that the total cell density $n_C(r)$:

$$n_C(r)=\int_0^{T_c} n(a,r)\,da+n_Q(r) \tag{7}$$

will satisfy the equation

$$\frac{1}{r}\frac{d}{dr}(run_C)=n(T_c,r). \tag{8}$$

Assuming $n_C(r)=\bar{n}_C$, the cell densities can be normalized to this constant value. Let $\nu(a,r)=n(a,r)/\bar{n}_C$ and $f_Q(r)=n_Q(r)/\bar{n}_C$. Since there is no cell flux across the vessel wall, and thus $u(r_0)=0$, from (8) it must be

$$ru(r)=\int_{r_0}^{r} z\nu(T_c,z)\,dz. \tag{9}$$

We note that the value of u at $r=R$, multiplied by the total cell density, would give the flux of cells per unit area entering the necrotic region, that is the number of cells that die in the unit time from a segment of cord having an outer surface of unit area.

Taking into account Eq. (9), ν and f_Q will satisfy the following equations:

$$\frac{\partial \nu}{\partial a}+\frac{1}{r}\frac{\partial}{\partial r}\Big(\int_{r_0}^{r} z\nu(T_c,z)\,dz\cdot\nu\Big)=0 \tag{10}$$

$$\nu(0,r)=2\theta(r)\nu(T_c,r) \tag{11}$$

and

$$\frac{1}{r}\frac{d}{dr}\Big(\int_{r_0}^{r} z\nu(T_c,z)\,dz\cdot f_Q\Big)=2(1-\theta(r))\nu(T_c,r). \tag{12}$$

The functions $f_P(r)=\int_0^{T_c}\nu(a,r)\,da$ and $f_Q(r)$ are the fractions of cycling cells (*i.e.* the growth fraction) and, respectively, of quiescent cells at position r. Note that ν and f_Q are independent of the measurement unit of r.

A solution (ν, f_Q) of Eqs. (10)-(12) having physical meaning is bounded, with $\nu(a,r) \geq 0$ and $f_Q(r) \geq 0$, and such that $f_P(r)+f_Q(r)=1$ (there always exists the trivial solution $\nu(a,r)=0$, $f_Q(r)=1$). Noting preliminarly that Eq. (10) is independent of Eq. (12), we observe that, if Eq. (10) has a solution bounded and positive, Eq. (12) will have only one bounded and non-negative solution given by

$$f_Q(r) = \frac{2\int_{r_0}^{r} z(1-\theta(z))\nu(T_c,z)\,dz}{\int_{r_0}^{r} z\nu(T_c,z)\,dz}\,. \tag{13}$$

Moreover, if $\nu > 0$ and $f_Q \geq 0$ are bounded solutions of Eqs. (10)-(12), then it is $f_P(r)+f_Q(r)=1$. In fact, since the function $f_P(r)+f_Q(r)$ must satisfy the equation

$$\frac{1}{r}\frac{d}{dr}(ru(f_P+f_Q)) = \nu(T_c,r)\,,$$

and Eq. (9) holds, f_P+f_Q will have the general form:

$$f_P(r)+f_Q(r) = \frac{c}{\int_{r_0}^{r} z\nu(T_c,z)\,dz} + \frac{\int_{r_0}^{r} z\nu(T_c,z)\,dz}{\int_{r_0}^{r} z\nu(T_c,z)\,dz}$$

and then the only bounded solution is $f_P(r)+f_Q(r)=1$.

A nontrivial solution of Eqs. (10)-(12) is easily found for $\theta(r)$ constant and equal to θ, $1/2 < \theta \leq 1$. It can be verified that in this case (10) has the positive solution, that does not depend on r, given by

$$\nu(a,r) = 2\theta\frac{\ln(2\theta)}{T_c}\exp(-\frac{\ln(2\theta)}{T_c}a) \tag{14}$$

and, from (13) it is $f_Q(r)=2(1-\theta)$.

For $\theta(r)$ not constant, a proof of the existence and uniqueness of a nontrivial solution of Eqs. (10)-(12) is not yet available (the problem is under study). However, a numerical solution of these equation can be obtained. We preliminarly observe that, if there exists $\nu(a,r)$ bounded and regular enough, by defining $\nu^0(a)=\lim_{r\to r_0}\nu(a,r)$ and rewriting Eq. (10) as

$$\frac{\partial\nu}{\partial a} + \nu(T_c,r)\nu + \big(\frac{1}{r}\int_{r_0}^{r} z\nu(T_c,z)\,dz\big)\frac{\partial\nu}{\partial r} = 0$$

we have

$$\lim_{r\to r_0}\frac{\partial\nu}{\partial a} = -\nu^0(T_c)\nu^0(a)$$

and then

$$\frac{d\nu^0}{da} = -\nu^0(T_c)\nu^0(a). \tag{15}$$

Moreover, from (11) it is

$$\nu^0(0) = 2\theta(r_0)\nu^0(T_c), \tag{16}$$

where $\theta(r_0)=\lim_{r\to r_0}\theta(r)$. Let $g^0=\nu^0(T_c)$. All the solutions of equations (15)-(16) are given by

$$\nu^0(a) = 2\theta(r_0)g^0\exp(-g^0a)$$

where g^0 is such that

$$g^0 = 2\theta(r_0)g^0 \exp(-g^0 T_c).$$

The above equation has always the root $g^0 = 0$ that gives $\nu^0(a) = 0$ for every a. This is the unique solution when $\theta(r_0)=0$ or $\theta(r_0)=1/2$. Otherwise, there exists also the root

$$g^0 = \frac{\ln(2\theta(r_0))}{T_c}$$

that gives therefore

$$\nu^0(a) = 2\theta(r_0)\frac{\ln(2\theta(r_0))}{T_c} \exp(-\frac{\ln(2\theta(r_0))}{T_c}a). \tag{17}$$

It is $\nu^0(a) > 0$ when $1/2 < \theta(r_0) \leq 1$, and thus the condition $\theta(r_0) > 1/2$ is necessary (and sufficient) for the non-zero $\nu^0(a)$ to be positive. This condition appears to be biologically meaningful, since it states that there exists a portion of the cord (at least near the vessel) in which the cell division originates a number of proliferating cells greater than the number of quiescent cells.

Equation (10) was solved numerically by means of a finite difference scheme that utilizes the condition given by Eq. (17), and an iterative procedure was used to satisfy the boundary condition (11). Figure 3 shows the profile of the age density function ν at three different radial positions for typical values of the cell cycle time and of the parameters of the cord (see the figure legend). The recycling probability $\theta(r)$ was assumed to decrease linearly from $\theta(r_0)=1$ to $\theta(R)=0.2$ to simulate the worsening of the environmental conditions when moving towards the periphery of the cord. Note that the integral of $\nu(a, r)$, *i.e.* the fraction of P cells at r, decreases as the radial distance increases. Figure 4 shows the pattern of the velocity u computed in the same conditions.

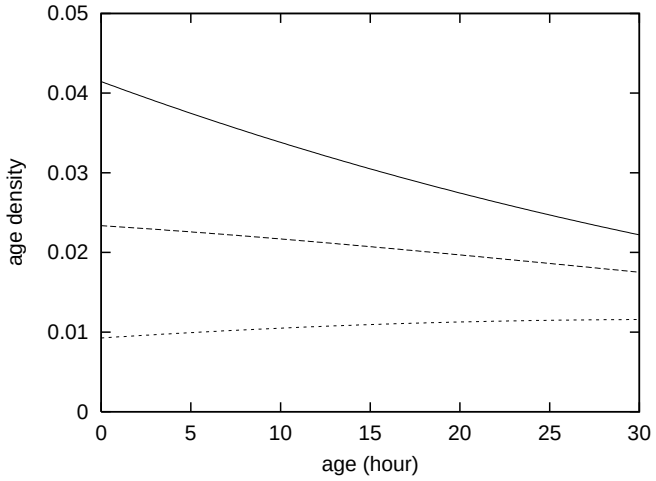

Fig. 3. Age density function $\nu(a, r)$ at various radial distances from the axis of the vessel: $r=1.5$ (continuous line), $r=3.5$ (dashed line), $r=5.5$ (dotted line). Cord parameters: $r_0=1$, $R=7$. Radial distances are normalized to r_0. Cell cycle time: 30 h. $\theta(r)$ decreases linearly from 1 to 0.2.

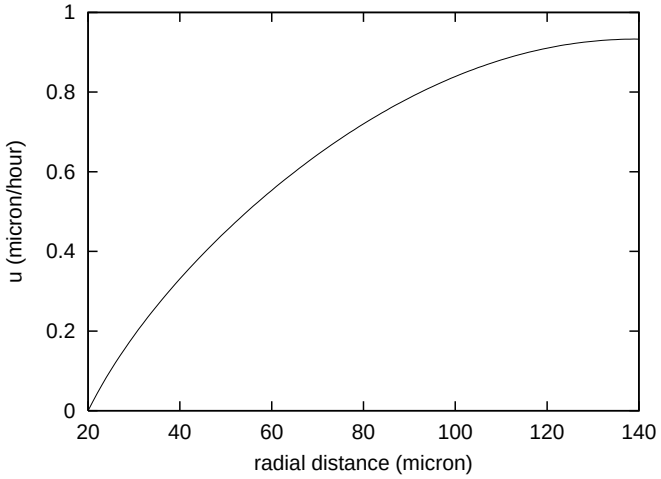

Fig. 4. Velocity $u(r)$ within the cord. The parameters are as in Fig. 3 and $r_0 = 20\,\mu$m.

4. Comparison with labelling experiments

The main experimental technique used to investigate the cell kinetics in tumour cords was based on the incorporation of tritiated thymidine, a radioactively labelled DNA-precursor, into the DNA synthesizing cells. After a short infusion of tritiated thymidine, that approximately performs as a pulse labelling, the fraction of labelled cells (LI, labelling index) gives the fraction of cells in S phase. In our model, the cells in S phase are those having age between T_{G1} and T_{G1}+T_S, where T_{G1} and T_S represent the duration of $G1$ and S phase, respectively. The labelling index of cells at position r is then given by

$$LI(r) = \int_{T_{G1}}^{T_{G1}+T_S} \nu(a, r)\, da\,. \tag{18}$$

The value of LI at different distances from the central vessel has been measured with a good resolution by Moore *et al.* (1984) in the cords of two rat hepatomas. For these two tumours the authors also gave the mean values of cord and vessel radius and the durations of cell cycle phases. By using these values and adjusting the form of the function $\theta(r)$ we were able to obtain a reasonable fitting of experimental data, see Fig. 5, except that for the inner regions of hepatoma 3924A. This discrepancy is likely to be caused by a decrease of the cycle time of cells when moving from the outer to the inner zones of the cord, whereas the published value of T_c is an average for the overall tumour.

An important measurement is the time evolution of the LI at a given spatial position. The experimental results indicate that the LI of the outer zone of the cord increases up to the value found initially in the inner zone. The time required for this increase has been taken as an estimate of the transit time of a cell cohort across the cord (Tannock, 1968; Hirst *et al.*, 1982; Moore *et al.*, 1984). We have computed the time course of LI after a tritiated thymidine pulse, assuming that at $t=0$ all the DNA-synthesizing cells become immediately labelled and that the cells born from labelled cells remain detectable as labelled. This last assumption is reasonable for 2-3 cell divisions. Let $\nu^l(a, r, t)$ be the age density function of labelled P cells and $f_Q^l(r, t)$ the

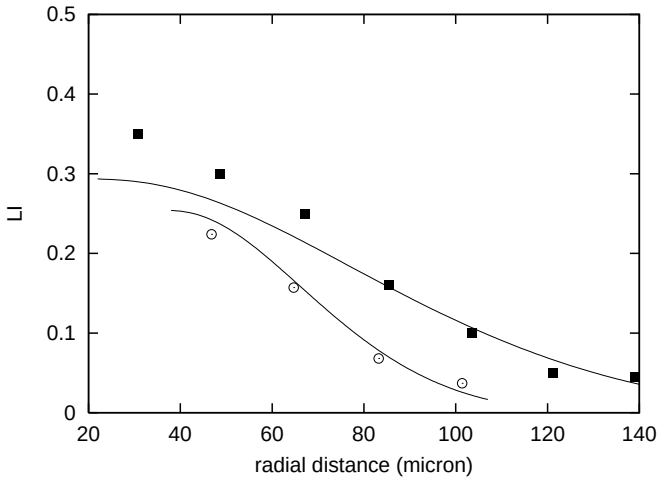

Fig. 5. Labelling index *vs.* radial distance. Experimental data (Moore *et al.*, 1984): 3924A hepatoma (squares), H-4-II-E hepatoma (circles); model predictions: continuous lines. Cord parameters of 3924A: $r_0 = 22\,\mu$m, $R = 140\,\mu$m, $T_c = 27.4\,$h, $T_S = 9.3\,$h, $T_{G2M} = 3.7\,$h; $\theta(r)$ was assumed equal to $1/(1+4[(r-r_0)/(R-r_0)]^2)$. Cord parameters of H-4-II-E: $r_0 = 38\,\mu$m, $R = 107\,\mu$m, $T_c = 17.2\,$h, $T_S = 6.6\,$h, $T_{G2M} = 3.8\,$h; $\theta(r)$ was assumed equal to $0.85/(1+4[(r-r_0)/(R-r_0)]^2)$.

fraction of labelled Q cells, at position r and time t after the pulse. In a cord at the stationary state, by writing the conservation laws, we have that these fractions obey for $t \geq 0$ the equations:

$$\frac{\partial \nu^l}{\partial t} + \frac{\partial \nu^l}{\partial a} + \frac{1}{r}\frac{\partial}{\partial r}(ru\nu^l) = 0 \tag{19}$$

$$\nu^l(0,r,t) = 2\theta(r)\nu^l(T_c,r,t) \tag{20}$$

$$\nu^l(a,r,0) = \chi_S(a)\nu(a,r) \tag{21}$$

$$\frac{\partial f_Q^l}{\partial t} + \frac{1}{r}\frac{\partial}{\partial r}(run_Q^l) = 2(1-\theta(r))\nu^l(T_c,r,t) \tag{22}$$

$$f_Q^l(r,0) = 0 \tag{23}$$

where $\chi_S(a) = 1$ for $T_{G1} \leq a \leq T_{G1} + T_S$ and zero elsewhere, $\nu(a,r)$ is the stationary age-density function of (labelled and unlabelled) P cells, solution of Eq. (10), and $u(r)$ is given by Eq. (9). The initial condition (21) expresses the fact that, immediately after the pulse, only S-phase cells are labelled.

The labelling index at position r and time t is given by

$$LI(r,t) = \int_0^{T_c} \nu^l(a,r,t)\,da + f_Q^l(r,t)\,, \tag{24}$$

and obviously $LI(r,0)$ is equal to the $LI(r)$ as given by (18). By integrating Eq. (19) with respect to age, and taking into account (20)-(23), we obtain for $LI(r,t)$ the following equation:

$$\frac{\partial LI}{\partial t} + \frac{1}{r}\frac{\partial}{\partial r}(ruLI) = \nu^l(T_c,r,t) \tag{25}$$

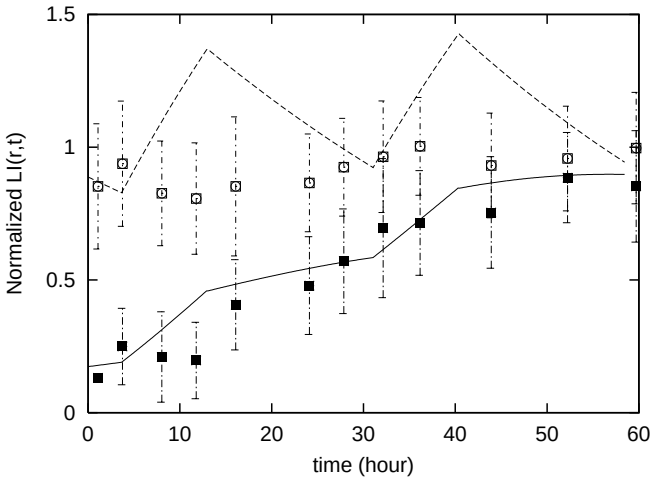

Fig. 6. Behaviour of $LI(r,t)/LI(r_1,0)$ at $r = 52\,\mu$m (dashed line) and $r = 132\,\mu$m (continuous line); $r_1 = 32\,\mu$m. Experimental data from the 3924A tumour (Moore *et al.*, 1984) are superimposed. Cord parameters and $\theta(r)$ as in Fig. 5.

with

$$LI(r,0) = \int_{T_{G1}}^{T_{G1}+T_S} \nu(a,r)\,da\,. \tag{26}$$

Note that a cell of age T_c at position r and time t is labelled if and only if its age at $t=0$ (or the age of one of its progenitors, if $t > T_c$) was between T_{G1} and $T_{G1}+T_S$, *i.e.* the cell (or its progenitor) was in S phase at $t=0$. Thus it is

$$\nu^l(T_c,r,t) = \chi^l(t)\nu(T_c,r) \tag{27}$$

where

$$\chi^l(t) = \begin{cases} 1, & \text{if } t \in (T_{G2M} + kT_c, T_{G2M} + T_S + kT_c), \quad k = 0,1,\cdots \\ 0, & \text{elsewhere.} \end{cases}$$

We have computed the solution of Eqs. (25)-(26), taking into account (27), by means of a finite difference scheme that uses the values of ν and u computed for the cord at the stationary state.

Using the parameters reported by Moore *et al.* (1984) for the hepatoma 3924A, and the function $\theta(r)$ selected in order to fit the LI data of Fig. 5, the time courses of LI at various distances from the central vessel were computed. Figure 6 shows the experimental data of the time behaviour of LI measured by Moore *et al.* (1984) in two $20\,\mu$m-wide zones of the cord, and the model predictions computed at the radial distances which are central for the two zones. The model predicts the overall increasing trend of LI in the outer zone, as experimentally observed. Less successful is the prediction of the model for the inner zone, where the computed behaviour exhibits marked oscillations and generally higher values. The introduction of cell-to-cell variability of cycle phase transit times could, however, dampen the oscillations. In particular, we predict that the LI of the outer zone reaches the initial value of the inner zone in about two cycle times, although the computed velocity u is always smaller than $1\,\mu$m/h. This indicates that the values of the migration velocity given in Tannock (1968), Hirst *et al.* (1982), and Moore *et al.* (1984) could be markedly overestimated.

5. Oxygen tension profile

The profile of oxygen tension along the cord radius has been computed by various authors (Thomlinson and Gray, 1955; Tannock, 1968; Moore *et al.*, 1984; Moore *et al.*, 1985) on the basis of a simple diffusion model (see also Vaupel, 1979), assuming a constant oxygen consumption rate per unit volume. The decay of oxygen tension along the cord radius could be important for determining the overall radiosensitivity of the cord. It is well-known indeed that hypoxic cells are less radiosensitive than well oxygenated cells (Tannock, 1972; Alper, 1979).

Our model could be useful for refining the computation of this profile because it could yield a more accurate description of the oxygen consumption rate by taking into account the possible differences in consumption between proliferating and quiescent cells (Bredel-Geissler *et al.*, 1992). As an example of this application, starting from the measured values of cord radius and vessel radius, we computed the profile of oxygen concentration and its value in the central vessel for the cords of the two rat hepatomas 3924A and H-4-II-E (Moore *et al.*, 1984).

If axial changes of O_2 concentration are neglected, for the oxygen concentration $\sigma(r)$, the following equation can be written:

$$\frac{D_{O2}}{r}\frac{d}{dr}\left(r\frac{d\sigma}{dr}\right) = A(r,\sigma) \qquad r_0 < r < R \tag{28}$$

with the boundary conditions

$$-\left.\frac{d\sigma}{dr}\right|_{r=r_0} = \frac{k}{D_{O2}}(\sigma_B - \sigma(r_0)) \tag{29}$$

$$\left.\frac{d\sigma}{dr}\right|_{r=R} = 0 \tag{30}$$

$$\sigma(R) = \sigma_d, \tag{31}$$

where A is the consumption rate per unit volume, D_{O2} is the diffusion coefficient, k is the permeability coefficient of the vessel wall, σ_B is the oxygen concentration in blood, and σ_d the value of the oxygen concentration at the boundary with the necrotic region. The case with $A = \text{const}$, $\sigma_d = 0$ and with the boundary condition $\sigma(r_0) = \sigma_B$ was considered in Tannock (1968), Moore *et al.* (1984), and Moore *et al.*, (1985). We have assumed that oxygen consumption decreases with O_2 concentration according to a Michaelis-Menten law (with constant K_M) (Casciari *et al.*, 1992), and that the consumption of quiescent cells, A_Q, is smaller than the consumption of proliferating cells, A_P. Thus the consumption rate can be represented by the following expression:

$$A(r,\sigma) = \left[A_P f_P(r) + A_Q(1 - f_P(r))\right]\frac{\sigma(r)}{K_M + \sigma(r)}, \tag{32}$$

where the growth fraction $f_P(r)$ is given by the solution $\nu(a,r)$ of Eqs. (10)-(12). Given the cord radius R, and fixing a value for σ_d, equation (28) can be integrated backward starting from conditions (30) and (31). Condition (29) then yields σ_B.

Figure 7 shows the computed oxygen tension profiles for the hepatomas considered, assuming for r_0 and R the experimental values, and for the other parameters the following values found in Vaupel (1979) and Casciari *et al.* (1992): $A_P = 3.2\,\text{ml}O_2/100\,\text{ml}\cdot\text{min}$, $A_Q = A_P/4$, $K_M =$

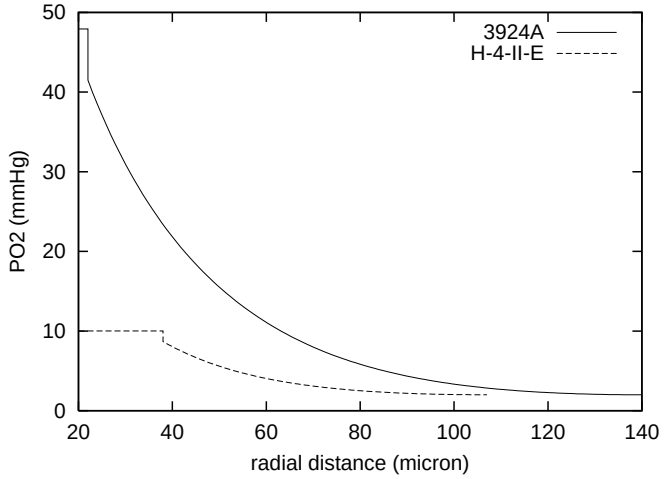

Fig. 7. Computed oxygen tension profiles for the cords of 3924A and H-4-II-E hepatomas. The parameter values are reported in the text.

4.55×10^{-6} M, $D_{O2} = 1.75\times10^{-5}$ cm^2/sec and $\sigma_d = 2$ mmHg. The ratio k/D_{O2} was approximated as the inverse of the thickness of the vessel wall and assumed equal to $0.25\,\mu\text{m}^{-1}$. As already computed by Moore *et al.* (1984), the oxygen tension in the blood vessel of the tumour H-4-II-E appears much smaller than in the other hepatoma. Using the Alper's formula for relative radiosensitivity (Alper, 1979), assuming that the ratio of the sensitivity of well oxygenated cells to the sensitivity of anoxic cells is equal to 2.75 and that the sensitivity halves at an O_2 tension of 7.5 mmHg, the relative radiosensitivity averaged on the 3924A cord was 1.66, whereas for H-4-II-E was 1.50. This result is in qualitative agreement with the response of the two hepatomas to radiations. To obtain realistic predictions, however, the values of the parameters used in Eqs. (28)-(32) should be assessed for the particular tumours considered, so that the preceding calculations have been presented only for illustrative purposes.

6. Possible variations in model equations

In this section we examine the consequences on model formulation of two variations in the basic assumptions of section 2.

First, we consider the effect of assuming constant in the cord the cell volume density, instead of the number of cells per unit volume. Let $\rho(r)$ be the cell volume density at the stationary state. It is

$$\rho(r) = \int_0^{T_c} v(a)n(a,r)\,da + v(0)n_Q(r) \tag{33}$$

where $v(a)$ is the volume of a cell of age a, with $v(T_c) = 2v(0)$. The volume of quiescent cells is assumed equal to $v(0)$. The physical meaning of ρ implies that it must be $\rho \leq 1$, and the ratio $\rho(r)/n_C(r)$ gives the mean volume of cells at position r. Multiplying Eq. (4) by $v(a)$, integrating with respect to age and taking into account condition (5), we obtain

$$\frac{1}{r}\frac{d}{dr}\Big(ru\int_0^{T_c} v(a)n(a,r)\,da\Big) = \int_0^{T_c}\frac{dv}{da}n(a,r)\,da - (1-\theta(r))v(T_c)n(T_c,r)\,.$$

Adding the above equation to Eq. (6) multiplied by $v(0)$, the following equation for $\rho(r)$ can be written:

$$\frac{1}{r}\frac{d}{dr}\left(ru\rho\right) = \int_0^{T_c} \frac{dv}{da} n(a,r)\, da\,. \tag{34}$$

By assuming $\rho(r)$ constant and equal to $\bar{\rho}$, from (34) it is

$$ru(r) = \frac{1}{\bar{\rho}} \int_{r_0}^{r} z \int_0^{T_c} \frac{dv}{da} n(a,z)\, da\, dz\,. \tag{35}$$

In the simple case of $v(a) = v_0 + (v_0/T_c)a$, Eq. (35) becomes

$$ru(r) = \frac{v_0}{\bar{\rho} T_c} \int_{r_0}^{r} z \int_0^{T_c} n(a,z)\, da\, dz\,, \tag{36}$$

showing the dependence of u on the number of proliferating cells per unit volume. Equations (35) or (36) should be substituted to Eq. (9) in Eqs. (4)-(6) in order to compute the cell densities $n(a,r)$ and $n_Q(r)$. Note that, in the case of cell volume linearly increasing with age, the mean cell volume of proliferating cells is equal to $v_0(1+<a>/T_c)$, where $<a>$ is the mean cell age. It can be easily seen that the mean cell volume in the cord will be always between v_0 and $v_0/\ln 2$, and thus the ratio of mean cell volume between inner and outer regions cannot exceed $1/\ln 2$. This fact suggests that the assumptions of constant cell volume density and constant number of cells per unit volume could lead in many cases to similar results, despite the different expressions of the velocity field.

We now consider the presence of some degree of random rearrangement of cells within the cord. Experiments of internalization of microspheres or labelled cells into multicellular spheroids (Dorie *et al.*, 1982; 1986) showed that the movement of the cell cohort towards the center of the spheroid was accompanied by spatial spreading, so suggesting the presence of some degree of diffusion. The presence of diffusion was taken into account by McElwain and Pettet (1993) in a mathematical model of this phenomenon. To incorporate the possibility of diffusive motions within the cord, we can assume that the flux of proliferating cells of age a per unit area, in the direction of r increasing across a cylindrical surface of radius r, is given by $-D\partial n(a,r)/\partial r + u(r)n(a,r)$ and the flux of quiescent cells by $-D dn_Q(r)/dr + u(r)n_Q(r)$, D being the diffusion coefficient. The conservation equations now become:

$$\frac{\partial n}{\partial a} + \frac{1}{r}\frac{\partial}{\partial r}(r[-D\frac{\partial n}{\partial r} + un]) = 0 \tag{37}$$

$$n(0,r) = 2\theta(r) n(T_c, r) \tag{38}$$

$$\frac{1}{r}\frac{d}{dr}(r[-D\frac{\partial n_Q(r)}{\partial r} + un_Q]) = 2(1-\theta(r))n(T_c,r), \tag{39}$$

and the condition of no cell flux across the vessel wall reads

$$\lim_{r\to r_0}(-D\frac{\partial n}{\partial r} + un) = 0$$

$$\lim_{r\to r_0}(-D\frac{dn_Q}{dr} + un_Q) = 0\,.$$

From Eqs. (37)-(39) we have that the total cell density n_C, as given by (7), will satisfy the equation

$$\frac{1}{r}\frac{d}{dr}(r[-D\frac{\partial n_C(r)}{\partial r}+un_C])=n(T_c,r)\,. \tag{40}$$

Assuming $n_C(r)$ constant and equal to $\bar{n}_C$, the no flux conditions at $r=r_0$ imply that $u(r_0)=0$ and thus, after introducing the normalized densities $\nu(a,r)$ and $f_Q(r)$ as in section 3, we have from (40)

$$ru(r)=\int_{r_0}^{r} z\nu(T_c,z)\,dz\,.$$

Therefore, ν and f_Q will satisfy the equations

$$\frac{\partial\nu}{\partial a}+\frac{1}{r}\frac{\partial}{\partial r}\Big(\int_{r_0}^{r} z\nu(T_c,z)\,dz\cdot\nu\Big)=\frac{1}{r}\frac{\partial}{\partial r}(rD\frac{\partial\nu}{\partial r}) \tag{41}$$

$$\nu(0,r)=2\theta(r)\nu(T_c,r) \tag{42}$$

and

$$\frac{1}{r}\frac{d}{dr}\Big(\int_{r_0}^{r} z\nu(T_c,z)\,dz\cdot f_Q\Big)=2(1-\theta(r))\nu(T_c,r)+\frac{1}{r}\frac{d}{dr}(rD\frac{df_Q}{dr})\,. \tag{43}$$

Note that, in this case, the migration of different cell subpopulations is no longer described by a unique velocity field. At a given radial position, the ratio between cell flux and cell density can be different for proliferating and quiescent cells, and, within P cells, is also depending on age.

7. Concluding remarks

In this paper we have proposed a model which describes the age structure of the cell population, and its spatial dependence, in a tumour cord at the stationary state. Cell migration was accounted for in a very simplified way, considering the cell population as a single continuous medium. Cell motions in the direction of the axis of the central vessel were disregarded, so that a scalar field of radial velocity was considered. The kinematics was thus specified by the laws of conservation of the number of cells. Cell motions of diffusive type were not considered here, but a suggestion as how to write the basic equations in the presence of some extent of diffusion is given in section 6. However, it appears difficult to assess the actual importance of diffusion in a tumour cord.

The cell cycle structure that was assumed does not allow for cell-to-cell variability of phase transit times (and then of cycle time) and for variations of cycle duration according to the spatial position of the cell. Although some experimental results seem to indicate a rather constant cycle transit time along the cord radius (Tannock, 1968), it appears indeed very likely (Hirst and Denekamp, 1979, Hirst *et al.*, 1982) that cells slow their progression in the cycle as they move towards the periphery of the cord, where the environmental conditions are worsening. Distributed cell cycle transit times and changes of these times with the radial position could be accounted for by considering an age-structured model with mitotic rate depending on age and position. In a simple view, the variability of the cell cycle could be restricted to G1 phase, as suggested by some experimental evidences. It is expected that the consideration of more realistic cell cycle structures could improve the model predictions of the data obtained by labelling experiments.

In the present model we disregarded cell death by apoptosis within the cord and assumed no recruitment of quiescent cells into the cycle. Both these phenomena can be easily incorporated in model equations by introducing appropriate rate constants. However, the presence of apoptosis and of the recruitment of quiescent cells was not considered in the present work since they seem mainly important when modelling the response to therapy.

Despite the above mentioned limitations, the model appears to capture the essential features of the proliferative behaviour of the tumour cords. The model could be useful to improve the computation of the oxygen tension profile along the cord radius (or the profile of the concentration of other substrates, as glucose), provided that the value of a certain number of parameters be estimated with reasonable accuracy. A precise determination of the oxygenation status of tumour cells is important to evaluate the responsiveness of the cord to radiation. It is known that tumour cords, after a single dose of radio or chemotherapy, undergo a shrinkage of the radius followed by a possible regrowth (Moore *et al.*, 1980; 1983). In these phenomena the different susceptibility of proliferating and quiescent cells to the therapeutic agent, the cell motility and the reentry into the cycle of quiescent cells can play an important role. Although the present work was confined to the study of the stationary state, it can be seen as the first step towards the modelling of the dynamics of corded tumours during therapy.

References

Adam J.A. and Maggelakis S.A., Diffusion regulated growth characteristics of a spherical prevascular carcinoma. *Bull. Math. Biol.* 52, 549-582 (1990).

Alper T., *Cellular Radiobiology.* Cambridge, University Press (1979).

Bredel-Geissler A., Karbach U., Walenta S., Vollrath L. and Mueller-Klieser W., Proliferation-associated oxygen consumption and morphology of tumour cells in monolayer and spheroid culture. *J. Cell. Physiol.* 153, 44-52 (1992).

Casciari J.J., Sotirchos S.V. and Sutherland R.M., Variations in tumor cell growth rates and metabolism with oxygen concentration, glucose concentration, and extracellular pH. *J. Cell. Physiol.* 151, 386-394 (1992).

Chaplain M.A.J., From mutation to metastasis: the mathematical modelling of the stages of tumour development. In: *A Survey of Models for Tumor-Immune System Dynamics* (Adam J.A. and Bellomo N., Eds.), Boston, Birkhäuser, pp. 187-236 (1997).

Danova M., Riccardi A. and Mazzini G., Cell cycle-related proteins and flow cytometry. *Haematologica* 75, 252-264 (1990).

Dorie M.J., Kallman R.F., Rapacchietta D.F., van Antwerp D. and Huang Y.R., Migration and internalization of cells and polystyrene microspheres in tumour cell spheroids. *Exp. Cell Res.* 141, 201-209 (1982).

Dorie M.J., Kallman R.F. and Coyne M.A., Effect of Cytochalasin B, Nocodazole and irradiation on migration and internalization of cells and microspheres in tumour cell spheroids. *Exp. Cell Res.* 166, 370-378 (1986).

Falkvoll K.H., The relationship between changes in tumour volume, tumour cell density and parenchymal cord radius in a human melanoma xenograft exposed to single dose irradiation. *Acta Oncol.* 29, 935-939 (1990).

Folkman J., Tumor angiogenesis. *Adv. Cancer Res.* 19, 331-358 (1974).

Folkman J., Tumor angiogenesis. *Adv. Cancer Res.* 43, 175-203 (1985).

Gandar P.W., Kelly K.E., Harris P.M. and Dellow D.W., Analysis of growth and cell proliferation in wool follicles. In: *Modelling Digestion and Metabolism in Farm Animals* (Robson A.B. and Poppi D.P., Eds.), Canterbury, New Zealand, Lincoln University, pp. 189.203 (1990).

Greenspan H.P., Models for the growth of a solid tumor by diffusion. *Stud. Appl. Math.* 51, 317-340 (1972).

Gurtin M.E., A system of equations for age-dependent population diffusion. *J. Theor. Biol.* 40, 389-392 (1973).

Gurtin M.E. and MacCamy R.C., On the diffusion of biological populations. *Math. Biosci.* 33, 35-49 (1977).

Hirst D.G. and Denekamp J., Tumour cell proliferation in relation to the vasculature. *Cell Tissue Kinet.* 12, 31-42 (1979).

Hirst D.G., Denekamp J. and Hobson B., Proliferation kinetics of endothelial and tumour cells in three mouse mammary carcinomas. *Cell Tissue Kinet.* 15, 251-261 (1982).

Hirst D.J., Hirst V.K., Joiner B., Prise V. and Shaffi K.M., Changes in tumour morphology with alterations in oxygen availability: further evidence for oxygen as a limiting substrate. *Br. J. Cancer* 64, 54-58 (1991).

McElwain D.L.S. and Ponzo P.J., A model for the growth of a solid tumor with non-uniform oxygen consumption. *Math. Biosci.* 35, 267-279 (1977).

McElwain D.L.S. and Pettet G.J., Cell migration in multicell spheroids: swimming against the tide. *Bull. Math. Biol.* 55, 655-674 (1993).

Moore J.V., Hopkins H.A. and Looney W.B., Dynamic histology of a rat hepatoma and the response to 5-fluorouracil. *Cell Tissue Kinet.* 13, 53-63 (1980).

Moore J.V., Hopkins H.A. and Looney W.B., Response of cell populations in tumor cords to a single dose of cyclophosphamide or radiation. *Eur. J. Cancer Clin. Oncol.* 19, 73-79 (1983).

Moore J.V., Hopkins H.A. and Looney W.B., Tumour-cord parameters in two rat hepatomas that differ in their radiobiological oxygenation status. *Radiat. Environ. Biophys.* 23, 213-222 (1984).

Moore J.V., Hasleton P.S. and Buckley C.H., Tumour cords in 52 human bronchial and cervical squamous cell carcinomas: Inferences for their cellular kinetics and radiobiology. *Br. J. Cancer* 51, 407-413 (1985).

Tannock I.F., The relation between cell proliferation and the vascular system in a transplanted mouse mammary tumour. *Br. J. Cancer* 22, 258-273 (1968).

Tannock I.F., Oxygen diffusion and the distribution of cellular radiosensitivity in tumors. *Br. J. Radiol.* 45, 515-524 (1972)

Thomlinson R.H. and Gray L.H., The histological structure of some human lung cancers and the possible implications for radiotherapy. *Br. J. Cancer* 9, 539-549 (1955).

Vaupel P., Oxygen supply to malignant tumors. In: Tumor Blood Circulation. Angiogenesis, Vascular Morphology and Blood Flow of Experimental and Human Tumors (Peterson H., Ed.), Florida CRC Press, pp. 143-169 (1979).

Warren B.A., The vascular morphology of tumors. In: Tumor Blood Circulation. Angiogenesis, Vascular Morphology and Blood Flow of Experimental and Human Tumors (Peterson H., Ed.), Florida CRC Press, pp. 1-45 (1979).